



## Kinetic study on non-isothermal crystallization in glassy materials: application to the $\text{Sb}_{0.12}\text{As}_{0.40}\text{Se}_{0.48}$ alloy

P.L. López-Alemaný, J. Vázquez\*, P. Villares, R. Jiménez-Garay

*Departamento de Física de la Materia Condensada, Facultad de Ciencias, Universidad de Cádiz, Apartado 40, 11510 Puerto Real (Cádiz), Spain*

Received 22 December 1998

### Abstract

A procedure has been developed for analyzing the evolution with time of the volume fraction crystallized and for calculating the kinetic parameters at non-isothermal reactions in materials involving formation and growth of nuclei. By means of this method, and considering the assumptions of extended volume and random nucleation, a general expression of the fraction crystallized has been obtained, as a function of the temperature in bulk crystallization. The kinetics parameters have been deduced, assuming that the crystal growth rate has an Arrhenius-type temperature dependence, and the nucleation frequency is either constant or negligible. The theoretical method described has been applied to the crystallization kinetics of glassy alloy  $\text{Sb}_{0.12}\text{As}_{0.40}\text{Se}_{0.48}$  with and without previous reheating. According to the study carried out, it is possible to state that the reheating did not cause the appearance of nuclei, but that the as-quenched material already contains a sufficient number of them. The phases at which the alloy crystallizes after the thermal process have been identified by X-ray diffraction. The diffractogram of the transformed material suggests the presence of microcrystallites of  $\text{Sb}_2\text{Se}_3$  and  $\text{AsSe}$ , remaining in a residual amorphous matrix. © 1999 Elsevier Science S.A. All rights reserved.

**Keywords:** Glassy semiconductor; Nucleation and crystal growth; Glass transition; Crystallization kinetics; As-quenched glass and reheated glass; Crystalline phases

### 1. Introduction

Traditionally, solid state physics has meant crystal physics. Solidity and crystallinity are considered as synonymous in texts on condensed matter. Yet one of the most active fields of solid state research in recent years has been the study of solids that are not crystals, solids in which the arrangement of the atoms lacks the slightest vestige of long-range order. The advances that have been made in the physics and chemistry of these materials, which are known as amorphous solids or glasses, have been widely appreciated within the research community. The last decades have seen a strong theoretical and practical interest in the application of isothermal and non-isothermal experimental analysis techniques to the study of phase transformations. While isothermal experimental analysis techniques are, in most cases, more definitive, non-isothermal thermoanalytical techniques have several advantages. The non-isothermal techniques have become particularly prevalent for determination of the thermal

stability of amorphous alloys and in the investigation of the processes of nucleation and growth that occur during transformation of the metastable phases in the glassy alloy as it is heated. These techniques provide rapid information on such parameters as glass transition temperature and activation energy over a wide range of temperatures [1,2]. In addition, the physical form and thermal conductivity as well as the temperature at which transformations occur in most amorphous alloys make these transformations particularly suited to analysis in a differential scanning calorimeter (DSC).

The study of crystallization kinetics in amorphous materials by differential scanning calorimetry methods has been widely discussed in the literature [2–5]. Many authors used the so-called Kissinger plot [3] or Ozawa plot [6] directly to examine the kinetics of crystallization of amorphous materials. These methods, however, cannot be directly applied to the crystallization of amorphous materials and the physical meaning of the activation energies thus obtained are obscure because the crystallization is advanced not by the nth order reaction but by the nucleation and growth process. On the other hand, some authors applied the Johnson–Mehl–Avrami (JMA) equation to the

\*Corresponding author. Tel.: +34-956-890966; fax: +34-956-834924.

E-mail address: wagner@merlin.eca.es (J. Vázquez)

non-isothermal crystallization process [7–13], Although sometimes they appeared to get reasonable activation energies, this procedure is not appropriate because the JMA equation was derived for isothermal crystallization [14].

In this work, a method is proposed for analyzing the non-isothermal crystallization kinetics on the basis of nucleation and crystal growth processes, and it is emphasized that the crystallization mechanism, such as bulk crystallization, should be taken into account for obtaining a meaningful activation energy. In addition, the present paper applies the proposed method to the analysis of the crystallization kinetics of the glassy alloy  $\text{Sb}_{0.12}\text{As}_{0.40}\text{Se}_{0.48}$ . From this analysis it is possible to state that the as-quenched material already contains a large number of nuclei. Finally, the crystalline phases corresponding to the crystallization process were identified by X-ray diffraction (XRD) measurements, using Cu  $K\alpha$  radiation.

## 2. Theoretical basis

### 2.1. Nucleation, crystal growth and volume fraction crystallized

The theoretical basis for interpreting DTA or DSC results is provided by the formal theory of transformation kinetics. This formal theory is largely independent of the particular models used in detailed descriptions of the mechanisms of transformation, and therefore it leads to an expression, which can be considered as general, for the equation of evolution of the volume fraction crystallized.

The above-mentioned theory considers the nucleation frequency per unit volume,  $I_v$ , which is related to the reciprocal of a mean value of the period  $\tau$  (the time in which an individual region is formed). Suppose that at time  $t = \tau$  the untransformed volume is  $V_a$ , and that between times  $t = \tau$  and  $\tau + d\tau$  a number  $I_v V_a d\tau$  of new regions are nucleated. The crystal growth rate, in general, is anisotropic. This rate in any direction can be then represented in terms of the principal growth velocities,  $u_i$  ( $i = 1, 2, 3$ ), in three mutually perpendicular directions. In these conditions the unidimensional growth in an elemental time,  $dt'$ , can be expressed as  $u_i dt'$ , and this growth for a finite time is  $\int_{\tau}^t u_i dt'$ . The volume of a  $b$  region originating at time  $t = \tau$  is then

$$v_{\tau} = g \prod_i \int_{\tau}^t u_i dt' \quad (1)$$

where  $g$  is a geometric factor, which depends on the shape of the growing crystal and the expression,  $\prod_i \int_{\tau}^t u_i dt'$  condenses the product of the integrals corresponding to the values of the above quoted subscript  $i$ .

During the initial stages of transformation, when  $V_b \ll$

$V_a$ , the nuclei are widely spaced, and its interference is negligible. Under these conditions, the transformed volume at time  $t$  resulting from regions nucleated between times  $\tau$  and  $\tau + d\tau$  is  $dV_b = I_v V_a v_{\tau} d\tau$ . However, in subsequent stages of the process, we must consider the mutual interference of regions growing from separate nuclei. When two such regions impinge on each other it is possible that the two regions develop a common interface, over which growth ceases, although it continues normally elsewhere. This happens in the most crystallization reactions.

During the time  $d\tau$ , when  $I_v V_a d\tau$  new transformed regions are nucleated, it may be also considered that  $I_v V_b d\tau$  regions would have nucleated in the transformed portion of the assembly, had not transformation previously occurred there. Accordingly it is possible to define an extended volume of transformed material,  $V_e$ , by the relationship

$$dV_e = v_{\tau} I_v (V_a + V_b) d\tau = v_{\tau} I_v V d\tau \quad (2)$$

where  $V$  is the volume of the whole assembly.

The extended volume can be visualized as a series of volume elements having the same limiting surface as the actual transformed volume but all growing 'through' each other. Some elements of the transformed volume are counted twice, other three times, and so on, in order to obtain the extended volume. It is possible now to find a relation between  $V_e$  and  $V_b$ . Consider any small random region, of which a fraction  $(1 - V_b/V)$  remains untransformed at time  $t$ . During a further time  $dt$ , the extended volume will increase by  $dV_e$ , and the true volume by  $dV_b$ . Of the new elements of volume which make up  $dV_e$ , a fraction  $(1 - V_b/V)$  on average will lie in the previously untransformed material, and thus contribute to  $dV_b$ , whilst the remainder of  $dV_e$  will be in the already transformed material. This result clearly follows only if  $dV_e$  can be treated as a completely random volume element, and it is for this reason that virtual nuclei have to be included in the definition of  $V_e$ . Bearing in mind the hypothesis of random nucleation it is possible to write the relation between  $V_b$  and  $V_e$  in the form

$$dV_b = (1 - V_b/V) dV_e = (1 - x) dV_e \quad (3)$$

where  $x = V_b/V$  is the volume fraction transformed. Differentiating this expression and substituting the result into Eq. (3), one obtains

$$dV_e = V \frac{dx}{1-x} \quad (4)$$

This equation is related to Eq. (2), and after the value for  $v_{\tau}$  from Eq. (1) has been included, one obtains

$$\frac{dx}{1-x} = g I_v \left( \prod_i \int_{\tau}^t u_i dt' \right) d\tau \quad (5)$$

When the crystal growth rate is isotropic,  $u_i = u$ , an

assumption which is agreement with the experimental evidence since in many transformations the reaction product grows approximately as spherical nodules, Eq.(5) can be written as

$$\frac{dx}{1-x} = 4\pi I_v \left( \int_{\tau}^t u_i dt' \right)^3 d\tau \quad (6)$$

In non-isothermal experiments of bulk crystallization with a quenched glass containing no nuclei and assuming that the nucleation frequency is practically constant and crystal growth rate has an Arrhenian temperature dependence,  $u = u_0 \exp(-E/RT)$ , Eq. (6) becomes

$$\begin{aligned} \frac{dx}{1-x} &= \frac{4\pi I_v u_0^3}{\beta^3} \left( \int_{T_\tau}^{T_t} \exp(-E/RT') dT' \right)^3 d\tau \\ &= \frac{C_1}{\beta^3} I_1^3 d\tau \end{aligned} \quad (7)$$

where  $T_\tau$  is the corresponding temperature at time  $\tau$ , and  $\beta = dT'/dt'$  is the heating rate.

Using the substitution  $y' = E/RT'$  the integral  $I_1$  is transformed to the relationship

$$I_1 = (E/R) \int_y^{y_\tau} \frac{e^{-y'}}{y'^2} dy' \quad (8)$$

which can be represented by a series, resulting in

$$I_1 = \frac{E}{R} \left[ -e^{-y'} y'^{-2} \sum_{k=0}^{\infty} \frac{(-1)^k (k+1)!}{y'^k} \right]_{y'}^{y_\tau} \quad (9)$$

Considering that in alternating series the error is less than the first term neglected and bearing in mind that in most crystallization reactions  $y' = E/RT' \gg 1$  (usually  $E/RT' \geq 25$ ), it is possible to use only the first term of this series, without making any appreciable error, and Eq. (9) becomes

$$I_1 = (E/R) e^{-y} \cdot y^{-2} \quad (10)$$

if it is assumed that  $T_\tau \ll T$ , so that  $y_\tau$  can be taken as infinity. This assumption is justifiable for any heating treatment that begins at a temperature where nucleation and crystal growth are negligible, i.e. below  $T_g$  (glass transition temperature) for most glass-forming systems [15].

Taking the logarithm of Eq. (10) leads to an expression that, in the range of values of  $y$ ,  $20 < y < 60$ , can be fitted very satisfactorily by a linear approximation, giving

$$\ln(e^{-y} y^{-2}) \approx -5.1202 - 1.052y \quad (11)$$

and therefore

$$I_1 \approx (E/R) e^{-5.1202} e^{-1.052y} = A_1 e^{-1.052y} \quad (12)$$

To illustrate the above mentioned fit, Fig. 1 shows the

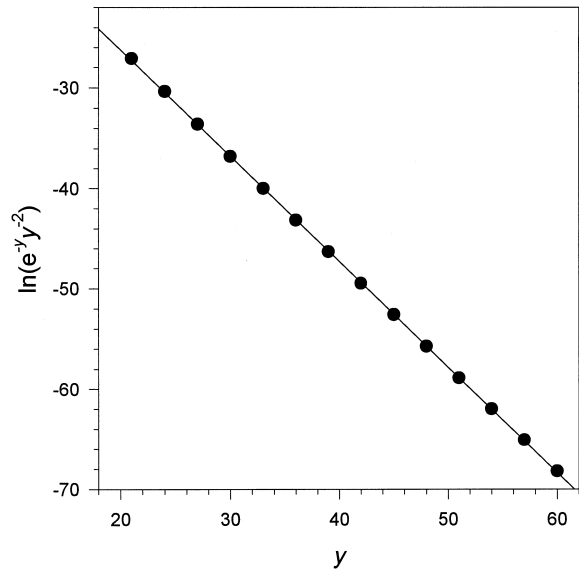


Fig. 1. Representation of  $\ln(e^{-y} y^{-2})$  versus  $y$  and corresponding straight regression line for the range of values  $20 < y < 60$ .

points  $(y, \ln(e^{-y} y^{-2}))$  together with the corresponding straight regression line.

Substituting Eq. (12) into Eq. (7) and integrating the resulting expression, one obtains

$$\begin{aligned} -\ln(1-x) &= \frac{C_2}{\beta^4} I_v (T - T_0) \exp(-1.052 \times 3E/RT) \\ &= \frac{C_2 N_0}{\beta^4} \exp(-1.052 \times 3E/RT) \end{aligned} \quad (13)$$

$N_0$  being the nuclei formed per unit volume in the course of the thermal process at the heating rate,  $\beta$ .

In the case of a glass which has been heated previously at the temperature of maximum nucleation rate for sufficiently long time, a large number of nuclei already exist and no new nuclei are formed during the thermal process (i.e.  $I_v = 0$ ), Eq. (6) can be written as

$$\frac{dx}{1-x} = 4\pi \left( \int_0^t u dt' \right)^3 dN = \frac{C_1}{\beta^3} I_2^3 dN \quad (14)$$

$dN$  being the number of nuclei in the elemental volume per unit volume, and where the integral has been evaluated between 0 and  $t$ , since there is no nucleation period,  $\tau=0$ .

The integral  $I_2$  has been resolved in the same manner as  $I_1$ , and substituting the resulting expression into Eq. (14), yields

$$\frac{dx}{1-x} = \frac{C_2^3}{\beta^3} \exp(-1.052 \times 3E/RT) dN$$

and therefore

$$-\ln(1-x) = \frac{C_2^3 N}{\beta^3} \exp(-1.052 \times 3E/RT) \quad (15)$$

Eqs. (13) and (15) may be expressed by the more general relationship

$$-\ln(1-x) = C_0 \beta^{-n} \exp(-1.052mE/RT) \quad (16)$$

Here,  $n = m + 1$  for a quenched glass containing no nuclei and  $n = m$  for a glass containing a sufficiently large number of nuclei. For diffusion-controlled growth,  $m$  assumes the values 1, 2 and 3 for one-, two- and three-dimensional growth, respectively.

## 2.2. Calculating kinetic parameters

The usual analytical methods, proposed in the literature for analyzing the crystallization kinetics in glass forming liquids, assume that the reaction rate constant can be defined by an Arrhenian temperature dependence. In order for this assumption to hold, one of the following two sets of conditions should apply:

1. The crystal growth rate,  $u$ , has an Arrhenian temperature dependence; and over the temperature range where the thermoanalytical measurements are carried out, the nucleation rate is either constant or negligible (i.e. the condition of site saturation).
2. Both the crystal growth and the nucleation frequency have Arrhenian temperature dependences.

In the present work the first condition is assumed, and therefore, the overall effective activation energy for crystallization is  $mE/n$ , where  $E$  is the activation energy of the crystal growth process. From this point of view, the crystallization rate is obtained by deriving the volume fraction crystallized with respect to time, and from Eq. (16) results

$$\frac{dx}{dt} = C_0 \beta^{-(n-1)} (1-x) \frac{1.052mE}{RT^2} \exp(-1.052mE/RT) \quad (17)$$

The maximum crystallization rate is found by making  $d^2x/dt^2 = 0$ , thus obtaining the relationship

$$\left(\frac{dx}{dt}\right)\bigg|_p = (1-x_p) \left\{ T_p^2 \left[ \frac{d}{dt} \left( \frac{1}{T^2} \right) \right]_p + 1.052mE\beta/RT_p^2 \right\} \quad (18)$$

where the subscript  $p$  denotes the magnitude values corresponding to the maximum crystallization rate.

Taking a sufficiently limited range of temperature (such as the range of crystallization peaks in DTA or DSC experiments), the fraction  $1/T^2$  can be considered practically constant, and therefore the Eq. (17) and (18) are transformed respectively into

$$\left(\frac{dx}{dt}\right)\bigg|_p = K_1 \beta^{-(n-1)} (1-x_p) \exp(-1.052mE/RT_p) \quad (19)$$

and

$$\left(\frac{dx}{dt}\right)\bigg|_p = 1.052mE\beta(1-x_p)/RT_p^2 \quad (20)$$

Relating both expressions and taking the logarithm leads to the relationship

$$\ln(T_p^2/\beta^n) = \frac{1.052mE}{R} \frac{1}{T_p} + \text{constant} \quad (21)$$

which represents a straight line whose slope yields the product  $mE$  of the process.

The use of Eq. (21) implies a previous knowledge of the kinetic exponent,  $n$ , which can be obtained taking the logarithm of Eq. (16), yielding

$$z = \ln[-\ln(1-x)] \\ = -n \ln \beta - 1.052mE/RT + \ln C_0 \quad (22)$$

and representing  $z$  versus  $\ln \beta$  at a specific temperature. The  $m$ -value should also be known, a parameter that depends on the dimensionality of the crystal. One method for determining the  $m$ -value is to observe the change of  $n$  with reheating at the nucleation temperature (slightly higher than the glass transition temperature,  $T_g$ ). If  $n$  does not change with reheating, a large number of nuclei already exists in the specimen and  $n = m$ . If  $n$  decreases with reheating, not so many nuclei exist in the specimen. In this case,  $m < n \leq m + 1$  before reheating and  $n = m$  after reheating.

Once the crystallization mechanism is precisely known and does not change with the heating rate, the plot of  $\ln(T_p^2/\beta^n)$  versus  $1/T_p$  gives the above-mentioned value of  $mE$ . Dividing  $mE$  by  $m$ , the activation energy for transformation can be obtained.

Finally, it should be noted that the change of  $\ln T_p^2$  with  $\beta$  is negligibly small compared with the change of  $\ln \beta^n$ , and, therefore, it is possible to write

$$\ln \beta^n = -\frac{1.052mE}{R} \frac{1}{T_p} + \text{constant} \quad (23)$$

This expression is often used to obtain the activation energy.

## 3. Experimental details

High purity (99.999%) antimony, arsenic and selenium in appropriate atomic percentage proportions were weighed into a quartz glass ampoule (6-mm diameter). The contents of the ampoule (7 g total) were sealed at a pressure of  $10^{-4}$  Torr ( $10^{-2}$  N m $^{-2}$ ) and heated in a rotating furnace at around 950°C for 24 h, submitted to a longitudinal rotation of 1/3 rpm in order to ensure the homogeneity of the molten material. It was immersed in a receptacle

containing water in order to solidify the material quickly, avoiding crystallization of the compound. The amorphous nature of the material was checked through a diffractometric X-ray scan, in a Siemens D500 diffractometer. The homogeneity and composition of the sample were verified through SEM in a JEOL, scanning microscope JSM-820. The thermal behavior was investigated using a Perkin-Elmer DSC7 differential scanning calorimeter. Temperature and energy calibrations of the instrument were performed, for each heating rate, using the well-known melting temperatures and melting enthalpies of high-purity zinc and indium supplied with the instrument. Powdered samples weighing about 20 mg (particle size around 40  $\mu\text{m}$ ) were crimped in aluminium pans, and scanned at room temperature through their glass transition temperature  $T_g$  at different heating rates: 2, 4, 8, 16, 32 and 64  $\text{K min}^{-1}$ . An empty aluminium pan was used as reference, and in all cases a constant flow of nitrogen, was maintained in order to extract the gases emitted by the reaction, which are highly corrosive to the sensory equipment installed in the DSC furnace. The  $T_g$  was considered as a temperature corresponding to the intersection of the two linear portions adjoining the transition elbow in the DSC trace, as shown in Fig. 2.

The crystallized fraction,  $x$ , at any temperature  $T$  is given by  $x = A_T/A$ , where  $A$  is the total area of the exotherm between the temperature  $T_i$  where the crystallization is just beginning and the temperature  $T_f$  where the crystallization is completed and  $A_T$  is the area between the initial temperature and a generic temperature  $T$ , see Fig. 2. With the aim of investigating the phases into which the samples crystallize, diffractograms of the material crystallized during DSC were obtained. The experiments were performed with a Philips diffractometer (type PW 1830). The patterns were run with Cu as target and Ni as filter ( $\lambda = 1.542 \text{ \AA}$ ) at 40 kV and 40 mA, with a scanning speed of  $0.1^\circ \text{ s}^{-1}$ .

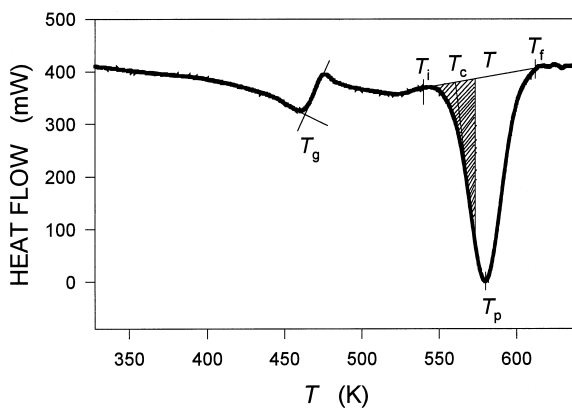


Fig. 2. Typical DSC trace of  $\text{Sb}_{0.12}\text{As}_{0.40}\text{Se}_{0.48}$  glassy alloy at a heating rate  $8 \text{ K min}^{-1}$ . The hatched area shows  $A_T$ , the area between  $T_i$  and  $T$ .

## 4. Results and discussion

The typical DSC trace of  $\text{Sb}_{0.12}\text{As}_{0.40}\text{Se}_{0.48}$  semiconductor glass obtained at a heating rate of  $8 \text{ K min}^{-1}$  and plotted in Fig. 2 shows three characteristic phenomena which are resolved in the temperature region studied. The first one ( $T = 465 \text{ K}$ ) corresponds to the glass transition temperature  $T_g$ , the second ( $T = 560 \text{ K}$ ) to the extrapolated onset crystallization temperature,  $T_c$ , and the third ( $T = 581 \text{ K}$ ) to the peak temperature of crystallization  $T_p$  of the above mentioned semiconductor glass. This behaviour is typical for a glass–crystal transformation. The values of  $T_g$ ,  $T_c$  and  $T_p$  increase with increasing the heating rate.

### 4.1. Glass transition

Two approaches are used to analyze the dependence of  $T_g$  on the heating rate. One is the empirical relationship of the form  $T_g = A + B \ln \beta$ , where  $A$  and  $B$  are constants for a given glass composition [16]. This was originally suggested and based on results for  $\text{Ge}_{0.15}\text{Te}_{0.85}$ . The results shown in Fig. 3 indicate the validity of this relationship for the  $\text{Sb}_{0.12}\text{As}_{0.40}\text{Se}_{0.48}$  alloy glass. For this glass, the empirical relationship can be written in the form

$$T_g = 489.3 + 8.42 \ln \beta$$

where a straight regression line has been fitted to the experimental data.

The other approach is the use of Eq. (21) with  $n = m = 1$ , for the evaluation of the activation energy  $E_g$  of the glass transition. For homogeneous crystallization with spherical nuclei, it has been shown [17,18] that the dependence of crystallization temperature on  $\beta$  is given by

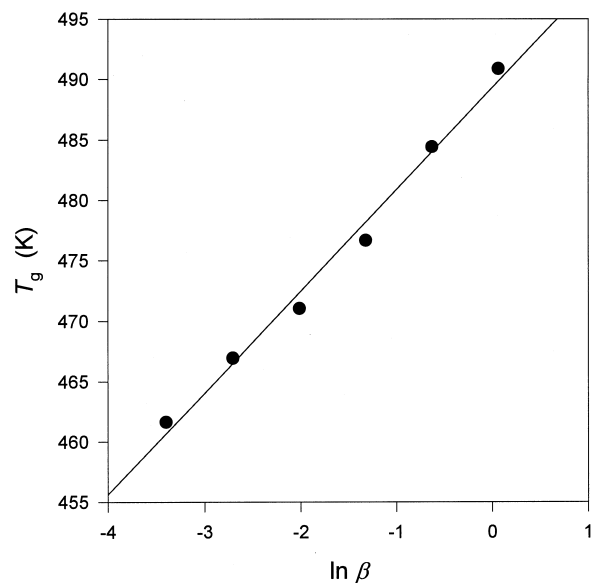


Fig. 3. Glass transition temperature versus  $\ln \beta$  ( $\beta$  in  $\text{K s}^{-1}$ ) of  $\text{Sb}_{0.12}\text{As}_{0.40}\text{Se}_{0.48}$  alloy.

$$\ln\left(\frac{T_c^2}{\beta}\right) = \frac{E}{R} \frac{1}{T_c} + \text{constant}$$

Though originally deduced for the crystallization process, it is suggested that this expression is valid in a very general sense [7], and it has often been used [17,19] to calculate  $E_g$ .

The activation energy for glass transition can also be evaluated from Eq. (23) with  $n = m = 1$ . It is therefore possible to write the above equation as

$$\ln \beta = -\frac{E_g}{R} \frac{1}{T_g} + \text{constant}$$

a straight line, whose slope yields a value of  $E_g$  and where the subscript g denotes magnitude values corresponding to the glass transition temperature.

Fig. 4 shows plots of  $\ln(T_g^2/\beta)$ , curve (a) and  $\ln \beta$ , curve (b) versus  $1/T_g$  for the  $\text{Sb}_{0.12}\text{As}_{0.40}\text{Se}_{0.48}$  semiconductor glass, displaying the linearity of the equations used. The values of the activation energy obtained for the glass transition are  $51.5 \text{ kcal mol}^{-1}$  (a) and  $53.4 \text{ kcal mol}^{-1}$  (b), respectively. The values obtained agree with the data quoted in the literature for similar compounds [20,21].

#### 4.2. Crystallization

The kinetic analysis of the crystallization reactions is related to the knowledge of the reaction rate constant as a function of the temperature. The usual analytical methods, proposed in the literature for describing the above-mentioned reactions, assume that the reaction rate constant can be defined by an Arrhenius type temperature dependence. Bearing in mind this assumption and that the nucleation

frequency is practically constant, as supposed in this work, the overall effective activation energy is related to the activation energy for crystal growth by the ratio  $m/n$ . From this point of view, and considering that in most crystallization processes the overall activation energy is much larger than the product  $RT$ , the crystallization kinetics of the alloy  $\text{Sb}_{0.12}\text{As}_{0.40}\text{Se}_{0.48}$  may be studied according to the appropriate approximation described in Section 2.

With the aim of analyzing the crystallization kinetics of the above mentioned alloy, the variation intervals of the magnitudes described by the thermograms, for the different heating rates, quoted in Section 3, are obtained and given in Table 1, where  $T_i$  and  $T_p$  are the temperatures at which crystallization begins and that corresponding to the maximum crystallization rate, respectively, and  $\Delta T$  is the width of the peak. The crystallization enthalpy  $\Delta H$  is also determined for each of the heating rates.

The area under the DSC curve is directly proportional to the total amount of alloy crystallized. The ratio between the ordinates and the total area of the peak gives the corresponding crystallization rates, which make it possible to plot the curves of the exothermal peaks represented in Fig. 5. It may be observed that the  $(dx/dt)_p$  values increase in the same proportion as the heating rate, a property which has been widely discussed in the literature [22].

With the aim of correctly applying the preceding theory, the material was reheated up to 536 K (a temperature slightly higher than  $T_g$ ) for 1 h in order to form a large number of nuclei. It was ascertained by X-ray diffraction that no crystalline peaks were detected after the nucleation treatment. From the experimental data the plots of  $z = \ln[-\ln(1-x)]$  versus  $\ln \beta$  at different specific temperatures have been drawn, both for the as-quenched glass and for the reheated glass. It has been observed that the correlation coefficients of the corresponding straight regression lines show a maximum value for a given temperature, which was considered as the most adequate one for the calculation of parameter  $n$ . Fig. 6 shows the relation between  $z$  and  $\ln \beta$  for as-quenched glass at 596.4 K and reheated glass at 579.3 K. According to Eq. (22), the slopes of these lines give the  $n$ -values, and it was found that  $n=2.1$  for the as-quenched glass and  $n=1.9$  for the reheated glass. Allowing for experimental error, both values are close to 2. This indicates that a large number of

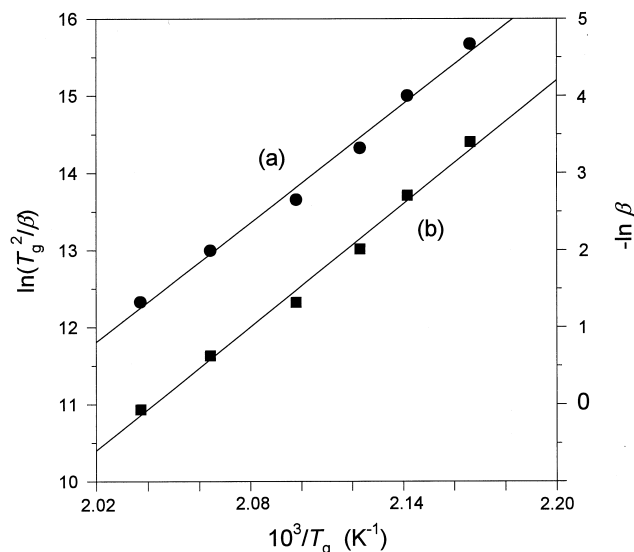


Fig. 4. (a) Plot of  $\ln(T_g^2/\beta)$  versus  $1000/T_g$  of the analyzed material. (b) Plot of  $\ln \beta$  versus  $1000/T_g$  of the studied glass ( $\beta$  in  $\text{K s}^{-1}$ ).

Table 1  
Characteristic temperatures and enthalpies of the crystallization process of the alloy  $\text{Sb}_{0.12}\text{As}_{0.40}\text{Se}_{0.48}$

Parameters	Experimental value	
	As-quenched	Reheated
$T_g$ (K)	459.2–490.9	433.9–484.0
$T_i$ (K)	553.7–598.8	527.7–575.5
$T_p$ (K)	579.2–641.4	551.6–618.1
$\Delta T$ (K)	51.1–73.0	51.8–80.0
$\Delta H$ (mcal $\text{mg}^{-1}$ )	4.1–5.1	2.0–2.9

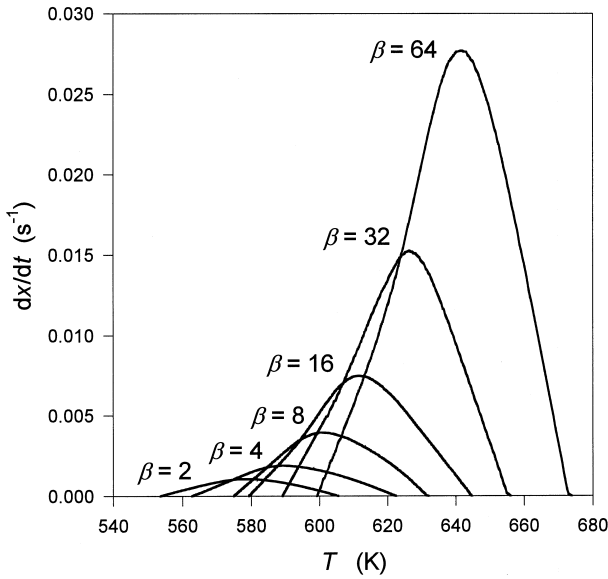


Fig. 5. Crystallization rate versus temperature of the exothermal peak at different heating rates.

nuclei exist already in the material, and therefore  $m=2$ , that is, the crystal particles grow two-dimensionally.

Once the crystallization mechanism is known, according to Eq. (21) it is possible to draw the plots in Fig. 7, which show the variation of  $\ln(T_p^2/\beta^n)$  with the reciprocal of the peak temperature. The slopes of these straight lines give the activation energy for crystal growth: 37.4 kcal mol<sup>-1</sup> for the reheated glass, and 38.0 kcal mol<sup>-1</sup> for the as-quenched glass. Also Eq. (23) has been used to obtain the above mentioned energy, and the results were 38.9 and 39.1 kcal mol<sup>-1</sup> for the material with and without previous reheating, respectively. It should be noted that the values

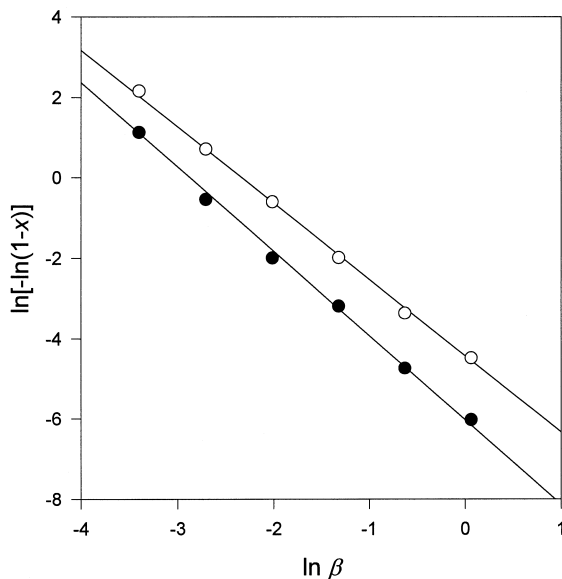


Fig. 6. Variation of  $\ln[-\ln(1-x)]$  with logarithm of heating rate ( $\beta$  in  $\text{K s}^{-1}$ ): ●, as-quenched glass, 596.4 K; ○, reheated glass, 579.3 K.

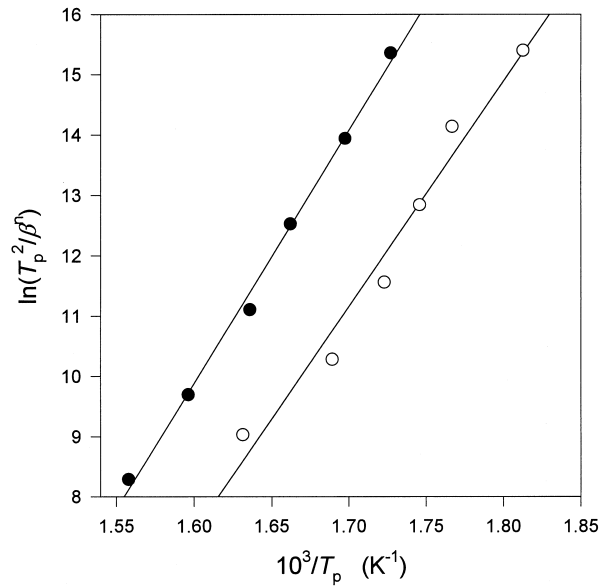


Fig. 7. Experimental plot of  $\ln(T_p^2/\beta^n)$  versus  $1000/T_p$  and straight regression lines of  $\text{Sb}_{0.12}\text{As}_{0.40}\text{Se}_{0.48}$  alloy ( $\beta$  in  $\text{K s}^{-1}$ ).

obtained from Eqs.(21) and (23) are very similar, which experimentally demonstrates that the change of  $\ln T_p^2$  with  $\beta$  is negligibly small compared with the change of  $\ln \beta$  as stated in the literature [15].

On the other hand, taking the logarithm of Eq. (16) one obtains the expression

$$\ln \beta = -1.052 \frac{m}{n} \frac{E}{RT} - \frac{1}{n} \ln [-\ln(1-x)] + \text{constant} \quad (24)$$

which permits representation of  $\ln \beta$  versus  $1/T$  for a specific value of the volume fraction crystallized. Fig. 8 shows the relation between  $\ln \beta$  and the reciprocal temperature at which  $x$  reaches 0.3 and 0.7. According to Eq. (24), this plot should give the  $E$  values, both for as-quenched glass and for reheated glass, which are shown in Table 2. Finally, by using Eq. (24), the relation between  $\ln \beta$  and  $1/T_p$  is shown in Fig. 9,  $T_p$  being the above-mentioned peak temperature in DSC curve. Since the volume fraction crystallized at  $T_p$  is practically the same irrespective of  $\beta$ , this plot should give the same information as Fig. 8. The activation energies thus obtained are also shown in Table 2.

It can be observed that the activation energies obtained from Eqs. (21) and (24) differ by only about 4.5%, which confirms that a large number of nuclei already exists in the specimen. Although it might be expected that the activation energy for the crystal growth would be less than the activation energy for the overall crystallization process, for the purpose of this alloy, the value obtained for the parameter  $n$  indicates that the reheating did not cause the appearance of nuclei, but that the as-quenched material already contains a sufficient number, so that both energies

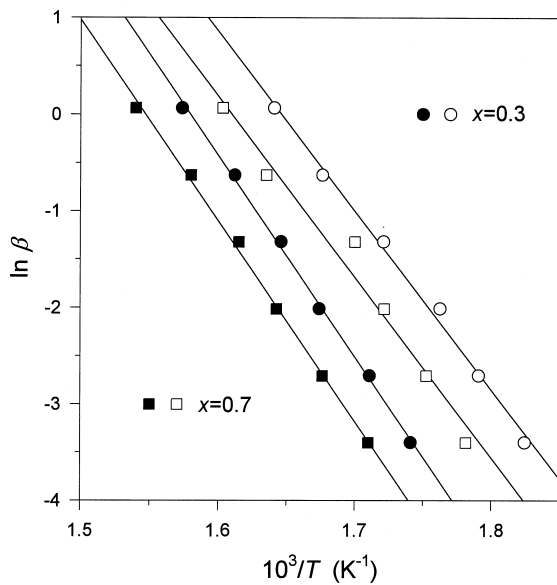


Fig. 8. Plot of  $\ln \beta$  versus  $1000/T$  for the values of the volume fraction crystallized equal to 0.3 and 0.7 ( $\beta$  in  $\text{K s}^{-1}$ ): ●, as-quenched glass; ○, reheated glass.

Table 2  
Activation energy obtained from the plot of  $\ln \beta$  versus  $1/T$  for given values of the volume fraction crystallized

Volume fraction crystallized	$E$ ( $\text{kcal mol}^{-1}$ )	
	As-quenched glass	Reheated glass
0.3	39.7	35.7
0.7	39.4	35.5
$x_p$	39.1	34.2

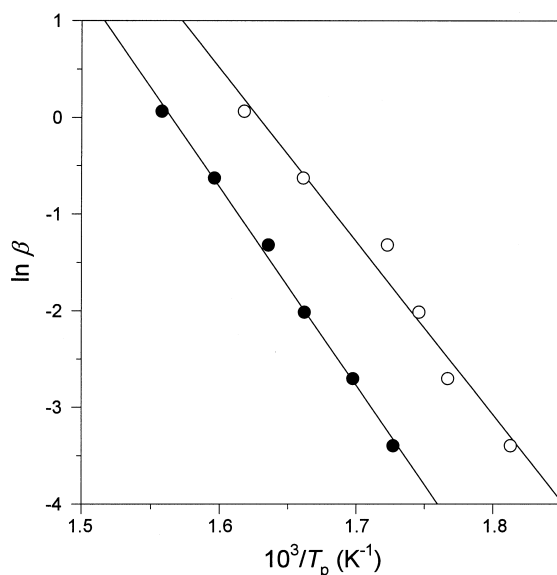


Fig. 9. Relation between  $\ln \beta$  and reciprocal of peak temperature in DSC curve ( $\beta$  in  $\text{K s}^{-1}$ ): ●, as-quenched glass; ○, reheated glass.

can be mutually identified because the crystallization process is basically a growth of the pre-existing nuclei.

From the mean value of the kinetic exponent  $\langle n \rangle = 2$ , and according to the Avrami theory of nucleation, it is possible to state the fact that in the crystallization reaction mechanism there is a diffusion controlled growth, coherent with the basic formalism used.

For the purpose of obtaining unambiguous conclusions on the crystalline growth morphology, the usual criteria for the interpretation of reaction order [23,24] have been used. According to these criteria, some observations relating to the morphology of the growth can be worked out. In the glassy alloy  $\text{Sb}_{0.12}\text{As}_{0.40}\text{Se}_{0.48}$  there is a relatively stable crystallization phase ( $\langle E \rangle = 39 \text{ kcal mol}^{-1}$ ), exhibiting a bulk nucleation mechanism and according to the literature [24] the crystalline phase may exhibit initial growth of particles nucleated at constant rate, since the mean value of the reaction order is included in the interval 1.5–2.5.

## 5. Identification of the crystalline phases

Taking into account the crystallization exothermal peaks shown by the glassy alloy  $\text{Sb}_{0.12}\text{As}_{0.40}\text{Se}_{0.48}$  it is recommended to try to identify the possible phases that crystallize during the thermal treatment applied to the samples by means of adequate XRD measurements. For this purpose, in Fig. 10 we show the most relevant portions of the diffractometer tracings for the as-quenched glass and for the material submitted to the thermal process. Fig. 10A has broad humps characteristic of the amorphous phase of the starting material at diffraction angles ( $2\theta$ ) between  $20^\circ$  and  $60^\circ$ . The diffractogram of the transformed material after the crystallization process (Fig. 10B) suggests the presence of microcrystallites of  $\text{Sb}_2\text{Se}_3$  and AsSe indicated with ● and ○, respectively, while there remains also a residual amorphous phase. The  $\text{Sb}_2\text{Se}_3$  phase found crystallizes in the orthorhombic system [25] with a unit cell defined by  $a = 11.633 \text{ \AA}$ ,  $b = 11.78 \text{ \AA}$  and  $c = 3.895 \text{ \AA}$ .

## 6. Conclusions

The described theoretical method enable us to study the evolution with the time of the volume fraction crystallized in materials involving nucleation and crystal growth processes. This procedure assumes the concept of the extended volume of transformed material and the condition of random nucleation. Using these assumptions we have obtained a general expression of the volume fraction crystallized, as a function of the temperature in bulk crystallization processes. In the quoted expression the numerical factors,  $n$  and  $m$  depend on the mechanism of nucleation and growth, and the dimensionality of the

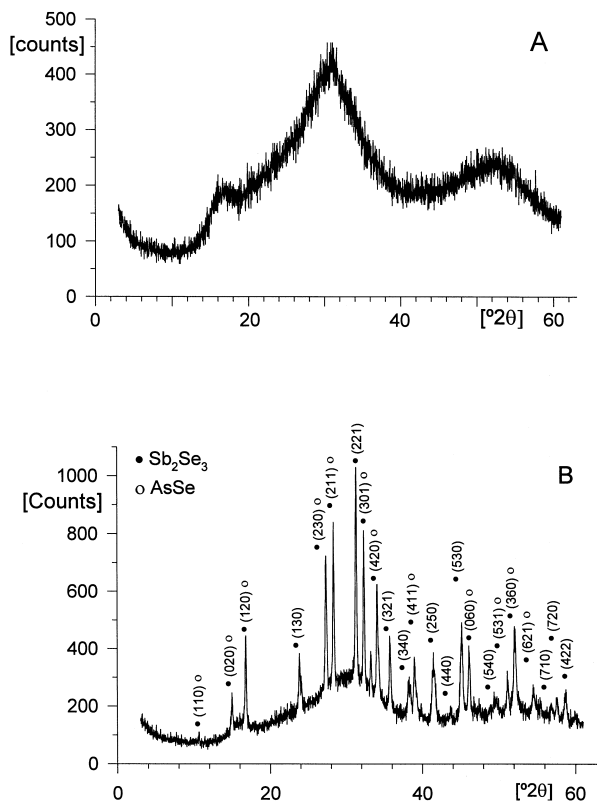


Fig. 10. (A) Diffractogram of amorphous alloy  $Sb_{0.12}As_{0.40}Se_{0.48}$ . (B) Diffraction peaks of alloy crystallized in DSC.

crystal. In addition,  $n = m + 1$  for a quenched glass containing no nuclei while  $n = m$  for a glass containing a sufficiently large number of nuclei. The kinetic parameters have been deduced by using the following considerations: the condition of the maximum crystallization rate and the mentioned maximum rate.

The theoretical method developed has been applied to the crystallization kinetics of the glassy alloy  $Sb_{0.12}As_{0.40}Se_{0.48}$  with and without previous reheating. According to the study carried out, it is possible to establish that the reheating did not cause the appearance of nuclei, but that the as-quenched material already contains a sufficient number of them. The method for thermal analysis of the quoted alloy has given results in good agreement with the nature of the material under study and representative of a crystal growth process, according to the value found for the kinetic exponent. In addition, two approaches were used to analyze the glass transition. One is the linear dependence of the glass transition temperature on the logarithm of the heating rate. The other is the linear

relationship between the logarithm of the quotient  $T_g^2/\beta$  and the reciprocal of the glass transition temperature. Finally, the identification of the crystalline phases was made by recording the X-ray diffraction pattern of the transformed material. This pattern shows the existence of microcrystallites of  $Sb_2Se_3$  and AsSe in an amorphous matrix.

## Acknowledgements

The authors are grateful to the Junta de Andalucía for financial support.

## References

- [1] Z. Altounian, J.O. Strom-Olsen, in: R.D. Shull, A. Joshi (Eds.), *Thermal Analysis in Metallurgy*, The Minerals, Metals and Materials Society, Warrendale, PA, 1992, p. 155.
- [2] D.W. Henderson, *J. Non-Cryst. Solids* 30 (1979) 301.
- [3] H.E. Kissinger, *Anal. Chem.* 29 (1957) 1702.
- [4] D.J. Sarrach, J.P. De Neufville, *J. Non-Cryst. Solids* 22 (1976) 245.
- [5] S. Surinach, M.D. Baro, M.T. Clavaguera-Mora, N. Clavaguera, *J. Non-Cryst. Solids* 58 (1983) 209.
- [6] T. Ozawa, *J. Thermal Anal.* 2 (1970) 301.
- [7] J. Colmenero, J.M. Barandiarán, *J. Non-Cryst. Solids* 30 (1979) 263.
- [8] J. Colmenero, J. Ilarraz, *Thermochim. Acta* 35 (1980) 381.
- [9] A. Marotta, A. Buri, F. Branda, S. Saiello, in: J.H. Simmons, D.R. Uhlmann, G.H. Beall (Eds.), *Advances in Ceramics, Nucleation and Crystallization in Glasses*, Vol. 4, The American Ceramic Society, Columbus, OH, 1982, p. 146.
- [10] A. Marotta, S. Saiello, F. Branda, A. Buri, *J. Mater. Sci.* 17 (1982) 105.
- [11] A. Lucci, L. Battezzati, C. Antonione, G. Riontino, *J. Non-Cryst. Solids* 44 (1981) 287.
- [12] E.M. Marseglia, *J. Non Cryst. Solids* 41 (1980) 31.
- [13] K. Harnisch, R. Lanzenberger, *J. Non-Cryst. Solids* 53 (1982) 235.
- [14] M.E. Fine, *Introduction To Phase Transformation in Condensed System*, Macmillan, New York, 1964, Ch. 3.
- [15] H. Yinnon, D.R. Uhlmann, *J. Non-Cryst. Solids* 54 (1983) 253.
- [16] M. Lasocka, *Mater. Sci. Eng.* 23 (1976) 173.
- [17] H.S. Chen, *J. Non-Cryst. Solids* 27 (1978) 257.
- [18] J.E. Shelby, *J. Non-Cryst. Solids* 34 (1979) 111.
- [19] J.A. Macmillan, *J. Phys. Chem.* 42 (1965) 3497.
- [20] M. Zhang, S. Manzini, W. Brezer, P. Boolchand, *J. Non-Cryst. Solids* 151 (1992) 149.
- [21] C.Y. Zahara, A.M. Zahara, *J. Non-Cryst. Solids* 190 (1995) 251.
- [22] Yi Qun Gao, W. Wang, F.Q. Zheng, X. Liu, *J. Non-Cryst. Solids* 81 (1986) 135.
- [23] R. Chiba, N. Funakoshi, *J. Non-Cryst. Solids* 105 (1988) 149.
- [24] C.N.R. Rao, K.J. Rao, *Phase Transition in Solids*, McGraw Hill, New York, 1978.
- [25] S.A. Dembovski, *Russ. J. Inorg. Chem. (Engl. transl.)* 8 (1963) 798.